

# Gadoxetic Acid-enhanced Magnetic Resonance Imaging and Contrast-enhanced Ultrasonography in the Diagnosis of Hepatocellular Carcinoma

CCM Cho

Department of Imaging and Interventional Radiology, Prince of Wales Hospital, Shatin, Hong Kong

## ABSTRACT

*Hepatocellular carcinoma (HCC) is the most common primary malignancy of the liver and one of the leading causes of cancer-related deaths. Early diagnosis of HCC is crucial to achieve good outcome. Advances in imaging technology enable detection of early disease, accurate tumour staging, treatment planning, and post-treatment monitoring, as well as an update of management guidelines. This review focuses on the development of gadoxetic acid-enhanced magnetic resonance imaging and contrast-enhanced ultrasonography in the diagnosis of HCC.*

**Key Words:** Carcinoma, hepatocellular; Gadolinium ethoxybenzyl DTPA; Magnetic resonance imaging; Sonazoid; Ultrasonography

## 中文摘要

### 釷塞酸增強磁共振成像和超聲造影的肝癌診斷

曹子文

肝細胞癌是肝臟中最常見的原發性惡性腫瘤，是癌症相關死亡的主要原因之一。及時診斷肝細胞癌是達至良好治療結果的關鍵。成像技術的進展有利於早期疾病檢測、準確腫瘤分期、治療計劃和治療後的監測，以及對治療指引的更新。本文重點回顧釷塞酸增強磁共振成像和超聲造影在診斷肝癌的進展。

## INTRODUCTION

Hepatocellular carcinoma (HCC) is the sixth most common cancer, accounting for >90% of all primary liver cancers.<sup>1</sup> Early diagnosis of HCC enables effective treatment and reasonable 5-year survival of 50% to 70%.<sup>2</sup> Risk factors for HCC include

chronic viral hepatitis infection, alcoholic and non-alcoholic fatty liver disease, and other types of chronic inflammatory liver diseases that lead to cirrhosis.<sup>3,4</sup> The risks of developing chronic hepatitis B and hepatitis C infections are 2.5% and 2% to 8% per year, respectively.<sup>5,6</sup> Before 2000, the diagnosis of HCC was

*Correspondence:* Dr CCM Cho, Department of Imaging and Interventional Radiology, Prince of Wales Hospital, 30-32 Ngan Shing Street, Shatin, Hong Kong. Email: ccm193@ha.org.hk

Submitted: 8 Mar 2017; Accepted: 10 May 2017.

Disclosure of Conflicts of Interest: All authors have disclosed no conflicts of interest.

made primarily by histopathological analysis. Advances in imaging and the risk of percutaneous biopsy (such as tumour seeding and bleeding) have resulted in an increased use of non-invasive methods. In 2001, the European Association for the Study of the Liver and the European Organisation for Research and Treatment of Cancer accepted non-invasive criteria based on a combination of imaging and laboratory findings for the diagnosis of HCC.<sup>7</sup> HCC is the only malignancy for which a radiological diagnosis is acceptable without histological confirmation.<sup>8</sup>

Gadoxetic acid-enhanced magnetic resonance imaging (Gd-EOB-MRI) and contrast-enhanced ultrasonography (CEUS) have gained popularity as the investigative tool of choice for HCC. Gadoxetic acid is a hepatocyte-specific contrast agent, commonly used in the detection and characterisation of hepatic lesions, particularly in patients at risk of developing HCC. Its sensitivity is superior to other modalities such as contrast-enhanced (CE) computed tomography (CT) and magnetic resonance imaging (MRI) with extracellular agents (ECA).<sup>9-12</sup>

For ultrasonography, second-generation contrast agents such as SonoVue (Bracco, Milan, Italy) and Sonazoid (GE Healthcare, Oslo, Norway) are most commonly used. They offer better diagnostic capability (than conventional grey-scale ultrasonography), safety profile (than iodinated or gadolinium chelate agents), and applicability in HCC management.<sup>13</sup>

## **GADOXETIC ACID-ENHANCED MAGNETIC RESONANCE IMAGING**

Gadoxetic acid possesses dual properties by providing information on both the vascular phase (during dynamic contrast enhancement) and hepatobiliary phase (HBP).<sup>14</sup> It has a higher affinity for protein binding and therefore an increased signal intensity during enhancement. While normal liver parenchyma progressively enhances due to the hepatocyte uptake of gadoxetic acid, most HCCs appear hypointense on the HBP. This leads to a greater lesion-to-liver contrast ratio and thus greater sensitivity in detecting small HCCs and greater specificity in differentiation from other focal liver lesions, and provides additional information on the multistep hepatocarcinogenesis process.<sup>15</sup> Early detection and treatment of HCCs can improve patient outcome.<sup>16,17</sup> Gd-EOB-MRI has also replaced fine-needle biopsy in the diagnosis of atypical lesions.<sup>18</sup>

## **Mechanism and Technique**

Gadoxetic acid is an ionic contrast medium with a linear molecular structure. Its enhancement effect is mediated by gadoxetate, an ionic complex formed by gadolinium and the ethoxybenzyl diethylenetriamine pentaacetic acid ligand (EOB-DTPA), which has a lipophilic property. Thus, gadoxetic acid possesses dual properties of extracellular and hepatobiliary proponents. After intravenous injection, Gd-EOB-DTPA distributes within the vessels and in the interstitial spaces during the dynamic enhancement phases (arterial phase, portovenous phase [PVP], and transition phase). After the PVP, progressive uptake of the contrast by normal hepatocytes peaks at approximately 20 to 40 minutes after injection. The contrast is eliminated by the renal and hepatobiliary tracts in similar amounts (50% each).<sup>19-21</sup> Biliary excretion typically commences after 10 minutes of injection in healthy individuals. The uptake by hepatocytes occurs through transport proteins in the sinusoidal membrane (organic anion-transporting polypeptide [OATP] 8, 1B1, and B3), and biliary excretion occurs through proteins in the canalicular membrane (MRP2) later. Gd-EOB-DTPA acts similarly to extracellular gadolinium chelates during the early dynamic enhancement phases, but it provides additional information during the HBP, during which normal hepatocytes concentrate the contrast medium while HCCs do not, resulting in a greater lesion-to-liver contrast ratio.<sup>22</sup>

Gd-EOB-DTPA has a high protein-binding capability and increases the T1 relaxivity. This produces superior enhancement and enables a reduction of dose as compared with other extracellular gadolinium-based contrast media.<sup>19,20,22</sup>

The recommended imaging protocols include non-contrast-enhanced sequences, T1-weighted in-phase and opposed-phase sequences, fast T2-weighted fat-saturated sequences, diffusion-weighted imaging (DWI), and pre-contrast T1-weighted fat-saturated sequences. These are followed by intravenous bolus injection of Gd-EOB-DTPA in a dose of 0.1 ml/kg (0.025 mmol/kg) at a rate of 1 ml/s, followed by saline solution flush (20 ml) at the same infusion rate. This corresponds to one-half of the dose of ECA usually used in abdominal studies. After injection, a T1-weighted fat-saturated gradient-echo sequence is obtained in the arterial phase (after 15-20 seconds), PVP (after 50-60 seconds), transition phase (after 120 seconds), and HBP (after 20 minutes). The total scan time may be reduced by

performing the T2-weighted sequence and the diffusion sequence between the transition phase and HBP.<sup>20,23,24</sup>

Gd-EOB-DTPA is well tolerated and is eliminated through the renal and hepatobiliary tracts. In patients with terminal renal dysfunction, it can be eliminated by dialysis. Nonetheless, there is still a possibility of nephrogenic systemic fibrosis despite the low exposure to gadolinium. Careful evaluation of risks and benefits is needed in patients with severe renal impairment. The compound does not cross the intact blood-brain barrier and diffuses through the placental barrier only in a small concentration. Data about exposure to Gd-EOB-DTPA during pregnancy are not available. No effect to the infant during breastfeeding is expected. Dose adjustment is not required in elderly patients or patients with hepatic or renal dysfunction. An increased bilirubin level is associated with a reduction in the enhancement effect in the liver during the HBP.<sup>21</sup>

Nonetheless, Gd-EOB-DTPA may be associated with hypersensitivity reactions or other idiosyncratic reactions characterised by cardiovascular, respiratory, or cutaneous manifestations, or shock. Its reported side-effects are similar to those of non-specific gadolinium chelates, including nausea (1%), headache (0.9%), lumbar pain (0.5%), vertigo (0.4%), vasodilation (0.6%), dysgeusia, and pain at the injection site.<sup>19,25</sup>

### **Detection of Small Hepatocellular Carcinoma**

Imaging diagnosis of small HCC ( $\leq 2$  cm) is a challenge,<sup>26</sup> as typical features of arterial hyperenhancement and washout are uncommon and overlap with other benign or premalignant lesions.<sup>27</sup> Small HCC may be subclassified as early and progressed HCC.<sup>28</sup> Histologically, early HCC is difficult to distinguish from high-grade dysplastic nodules. The presence of stromal invasion is the key to diagnosis. Early HCC consists of well-differentiated tumour cells that grow by replacement and thus has a vaguely nodular appearance with an indistinct margin. Progressed HCC consists of moderately differentiated tumour cells with an expansile growth pattern and thus has a discrete nodular appearance with a tumour capsule.<sup>29</sup>

In a meta-analysis of patients with chronic liver disease, the per-lesion sensitivity was significantly lower in subcentimetre HCC than larger HCC on CT (31% vs. 82%) and MRI (48% vs. 88%). Gd-EOB-MRI has a higher sensitivity than CECT in detecting HCC because of a higher lesion-to-liver contrast ratio

(Figure 1). Gd-EOB-MRI can detect additional HCCs in patients initially diagnosed as having a single lesion on dynamic CT.<sup>30</sup> Accurate detection can reduce the risk of recurrence and improve overall survival. Gd-EOB-MRI is superior to CT or ECA-MRI in detecting small HCCs.<sup>30</sup> A combination of Gd-EOB-MRI and DWI has even higher sensitivity in detecting small HCCs than either method alone.<sup>31,32</sup>

### **Hepatocellular Carcinoma Versus Dysplastic Nodule**

In cirrhotic livers, atypical enhancement patterns in small HCCs are not uncommon. It is difficult to differentiate early HCC from a non-malignant or premalignant dysplastic nodule owing to overlapping pathological and radiological features.<sup>33</sup> The HBP of Gd-EOB-MRI can be used to distinguish between the two (Figure 2). As OATP expression decreases during hepatocarcinogenesis, HCC is hypointense to background liver parenchyma on the HBP.<sup>34,35</sup> Signal intensities on DWI and HBP are useful to differentiate between HCC and dysplastic nodule, and between high-grade and low-grade dysplastic nodules.<sup>36</sup> HCC and a lesser proportion of high-grade dysplastic nodules are hyperintense on DWI, whereas low-grade dysplastic nodules are not.<sup>36</sup>

Hyperintensity on the HBP is suggestive of benign hepatocellular lesions such as focal nodular hyperplasia. Most HCCs are hypointense on HBP, though 5% to 20% of HCCs are iso- to hyper-intense on HBP due to genetic mutations, which cause a paradoxical over-expression of OATP, most commonly in moderately differentiated HCC.<sup>37,38</sup> Common features of hyperintense HCC on HBP include focal geographic defects of contrast uptake (indicating intratumoural necrosis or heterogeneous histological differentiation) and a hypointense rim (indicating a peritumoural capsule).<sup>39</sup>

### **Hepatocellular Carcinoma Versus Vascular Pseudolesion**

Vascular pseudolesions are non-tumourous perfusion alterations (such as arteriportal shunts) and can mimic small HCC. As cirrhosis progresses, sinusoidal capillarisation and obliteration of hepatic venules lead to arteriportal shunting.<sup>40</sup> These shunts usually appear as subcapsular wedge-shaped transient parenchymal enhancement on the arterial phase. In cirrhotic livers, the shunts typically have a centrally located, round or oval appearance due to architectural distortion of

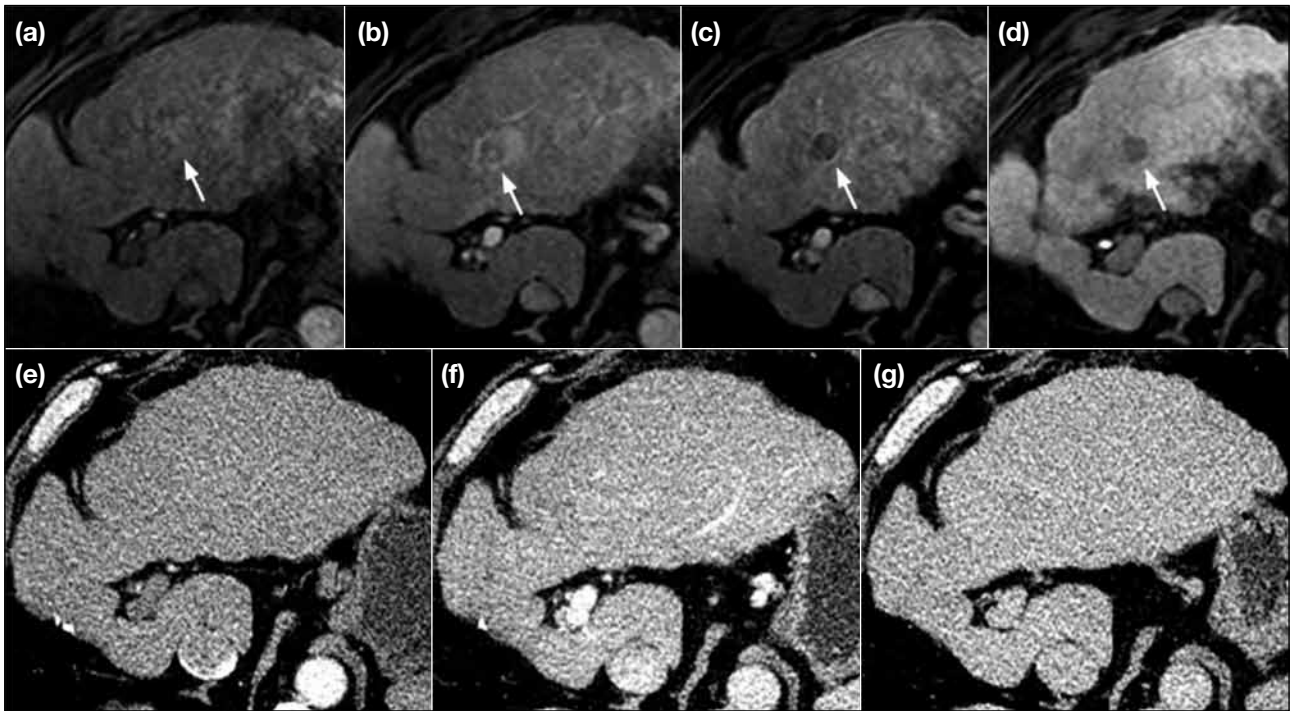


**Figure 1.** Gadoxetic acid-enhanced magnetic resonance imaging of the liver showing a 9-mm hepatocellular carcinoma in segment IVb (arrows), with very subtle hyperenhancement in the (a) early arterial phase, capsule enhancement and washout in the (b) portovenous phase, distinct hypoenhancement in both the (c) transitional and (d) hepatobiliary phases. Contrast-enhanced computed tomography showing near isoenhancement of the lesion in the (e) arterial, (f) portovenous, and (g) delayed phases.

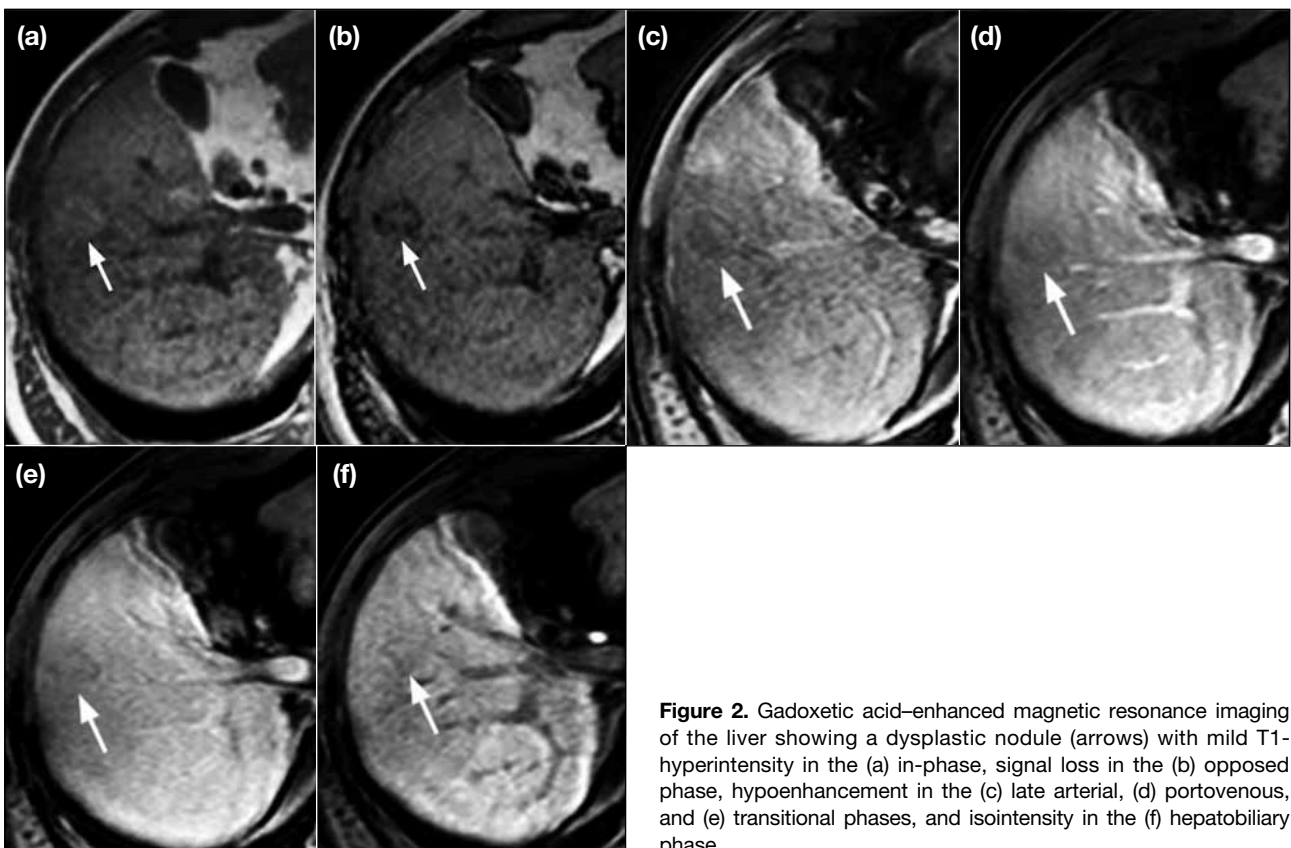


**Figure 2.** Gadoxetic acid-enhanced magnetic resonance imaging of the liver showing a dysplastic nodule (arrows) with mild T1-hyperintensity in the (a) in-phase, signal loss in the (b) opposed phase, hypoenhancement in the (c) late arterial, (d) portovenous, and (e) transitional phases, and isointensity in the (f) hepatobiliary phase.

the background parenchyma.<sup>41</sup> On Gd-EOB-MRI, vascular pseudolesion is typically isointense on the HBP due to intact hepatocyte function, whereas most small hypervascularised HCCs are hypointense on HBP (Figure 3). Nonetheless, >10% of vascular pseudolesions are relatively hypointense on HBP, it is suggested that low lesion-to-liver signal intensity ratio on the HBP and hyperintensity on DWI are more likely to indicate HCC than vascular pseudolesion.<sup>42</sup>

### Hepatocellular Carcinoma Versus Non-hepatocellular Tumours

Patients with chronic hepatitis and cirrhosis are at risk of developing intrahepatic cholangiocarcinoma (ICC), which is the second commonest primary hepatic malignancy after HCC. Differentiating ICC from HCC is crucial as their management and prognoses are different.<sup>43,44</sup> On CECT or ECA-MRI, ICC typically shows peripheral or weak enhancement on the arterial

phase and centripetal or persistent enhancement on the PVP and delayed phases.<sup>45,46</sup> Nonetheless, small ICCs in patients with cirrhosis display arterial enhancement and / or venous washout more frequently than those in the normal liver.<sup>47,48</sup> On Gd-EOB-MRI, both ICC and HCC are hypointense on HBP due to the lack of functioning hepatocytes.<sup>49</sup> On Gd-EOB-MRI, features suggestive of ICC include the absence of fat or capsule appearance, central hypointensity on T2-weighted images, lesser degree of arterial enhancement, and target appearance on DWI and HBP images (Figure 4).<sup>50-52</sup>

Imaging features of metastases vary according to the primary histology. Hepatic metastases from adenocarcinoma (such as colorectal cancer) are usually hypovascular and have arterial rim-like enhancement, whereas metastases from neuroendocrine tumour, renal cell carcinoma, melanoma, and breast cancer are hypervascular and have arterial enhancement

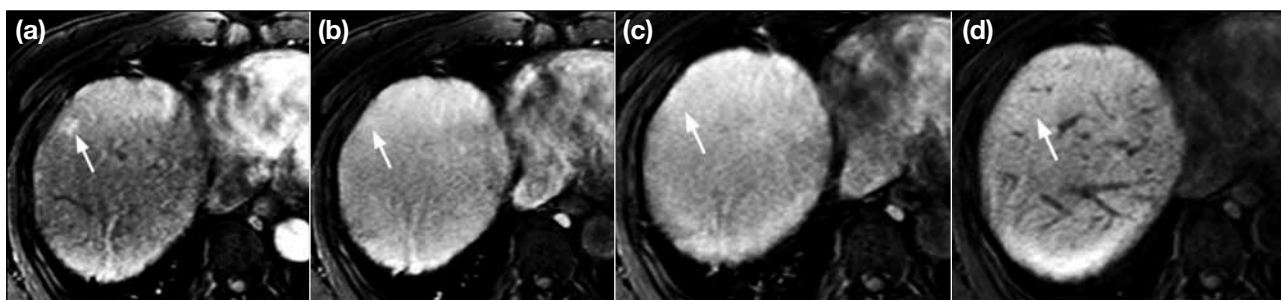


**Figure 3.** Gadoxetic acid-enhanced magnetic resonance imaging of the liver showing a vascular pseudolesion (arrows) with vague hyperenhancement in the (a) arterial phase and subsequent isoenhancement in the (b) portovenous, (c) transitional, and (d) hepatobiliary phases.

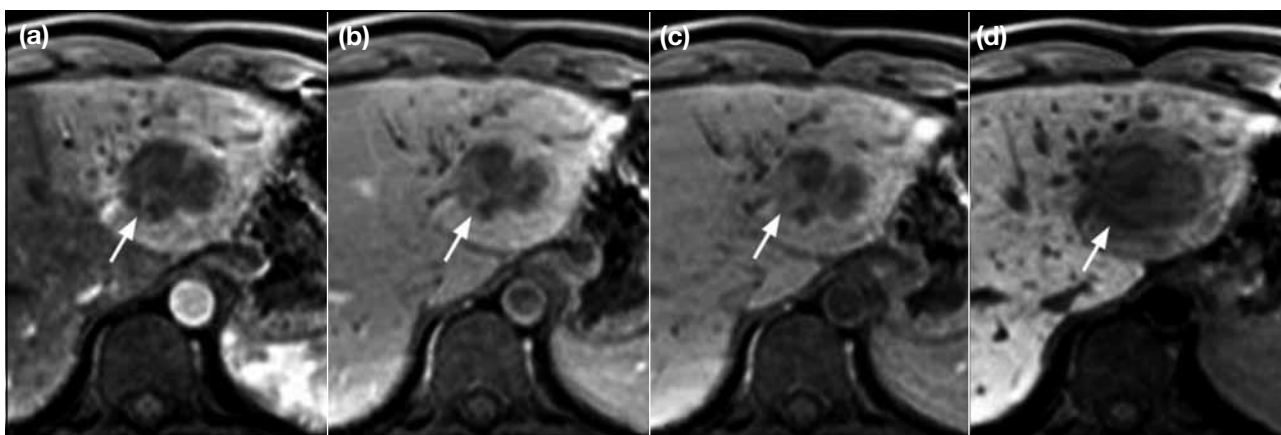


**Figure 4.** Gadoxetic acid-enhanced magnetic resonance imaging of the liver showing an intrahepatic cholangiocarcinoma (arrows), with subtle peripheral enhancement and arteriportal shunting with large perfusion alteration in the left lobe in the (a) arterial phase, centripetal enhancement in the (b) portovenous and (c) delayed phases, and a target appearance with hypointense rim in the (d) hepatobiliary phase.

with delayed washout, like HCC. Regardless of the primary histology, metastases are commonly identified as hypointense lesions on HBP images, owing to the lack of functioning hepatocytes within the tumour.<sup>53</sup> Thus, Gd-EOB-MRI may not be superior to CECT or ECA-MRI in differentiating metastasis from HCC. Nonetheless, metastasis is more likely in the presence of multiple focal lesions in a non-cirrhotic liver, especially in patients with known malignancy.<sup>54</sup>

Haemangioma is the most common benign hepatic pathology. On CECT and ECA-MRI, a typical haemangioma shows early peripheral nodular enhancement with subsequent centripetal and prolonged enhancement. On Gd-EOB-MRI, haemangioma is typically hypointense on HBP because of the absence of hepatocytes,<sup>55</sup> and of low signal intensity on the transition phase as the parenchymal enhancement gradually increases after the PVP, which is known as pseudowashout (Figure 5). According to the Liver Imaging-Reporting and Data System (LI-RADS) guidelines, washout should be determined in the PVP only and not in the transition phase.<sup>11</sup> Haemangiomas are typically moderately to markedly hyperintense on T2-weighted images and hyperintense on DWI with high apparent diffusion coefficient.<sup>56,57</sup>

Hepatic angiomyolipoma is a rare benign mesenchymal tumour and comprises variable proportions of thick-walled vessels, smooth muscle cells, and adipose tissue. It has diverse imaging features and mimics HCC to show arterial enhancement, intralesional fat, and washout.<sup>58,59</sup> In addition, lipid-poor angiomyolipoma has no detectable fat component on imaging or

chemical shift imaging.<sup>58,60</sup> On Gd-EOB-MRI, both entities show similar dynamic enhancement patterns, but angiomyolipoma tends to be more homogeneously hypointense and of lower signal intensity in HBP, as it does not contain hepatocytes, whereas HCC contains hepatocytes with various degrees of malignant change.<sup>61</sup>

### Gd-EOB-MRI Versus Other Modalities

Gd-EOB-MRI provides higher per-lesion accuracy for HCC diagnosis than CECT, CT hepatic arteriography, CT arteriportography, and ECA-MRI.<sup>62-64</sup> It provides maximum lesion conspicuity for HCC,<sup>35,65,66</sup> and characterises atypical HCCs.<sup>35,67-69</sup> It adds value in HCC diagnosis when combined with other imaging modalities.<sup>35,68,70-74</sup> Gd-EOB-MRI is more cost-effective than ECA-MRI or CECT; its direct costs are lower and can generate more quality-adjusted life years.<sup>75</sup>

### Gd-EOB-MRI as a Biomarker

HCC that is hyperintense on HBP has a higher grade of tumour differentiation and vice versa.<sup>76-80</sup> HCC with iso- / hyper-enhancement on HBP has a lower risk for vascular invasion and recurrence,<sup>81-83</sup> and lower levels of expression of poor-prognostic immunohistochemical / progenitor cell markers including alpha-fetoprotein, protein induced by vitamin K absence or antagonist II, epithelial cell adhesion molecule, cytokeratin 10, and glypican-3.<sup>18,82,84</sup> Signal intensity, morphology, and signal heterogeneity in HBP are poor prognosticators.<sup>85,86</sup>

For hypovascular nodules on dynamic imaging, hypointensity on HBP indicates high-risk lesions that later transform into overt hypervascular HCC.<sup>87-92</sup> The presence of hypovascular HBP hypointense nodules

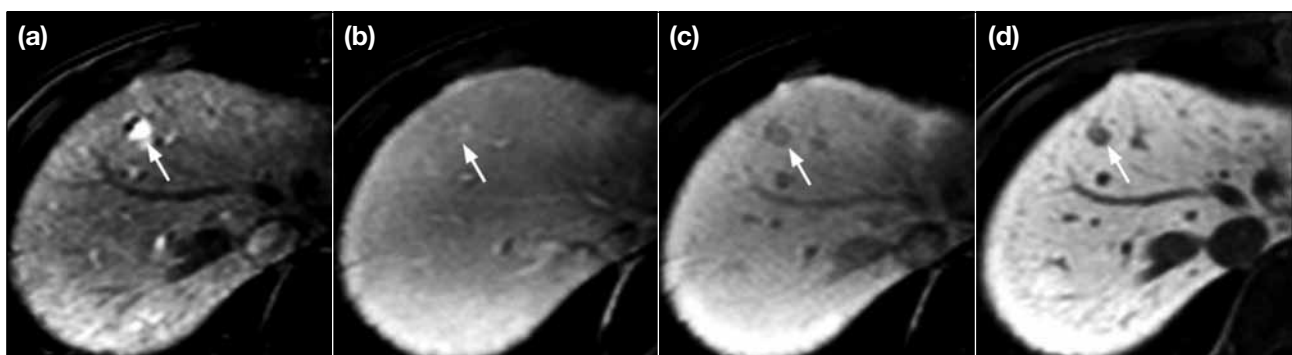


**Figure 5.** Gadoteric acid-enhanced magnetic resonance imaging of the liver showing a hepatic haemangioma at segment VIII (arrows), with peripheral nodular hyperenhancement in the (a) arterial phase, contrast fill-in in the (b) portovenous phase, hypoenhancement or pseudowashout in the (c) transitional phase, and hypointensity in the (d) hepatobiliary phase.

predicts multi-centric recurrence after resection.<sup>93</sup>

## CONTRAST-ENHANCED ULTRASONOGRAPHY

Colour and power Doppler ultrasonography have a low signal-to-noise ratio and thus can only depict blood flow in relatively large vessels and cannot detect intralesional vascularity.<sup>94</sup> Conventional ultrasonography is limited in diagnosis of HCC, as it depends on a characteristic vascular enhancement pattern. Ultrasound contrast agents can overcome this limitation.

Ultrasound contrast agents consist of microbubbles containing air or various gases within a shell. When administered into the vasculature, the agents enhance the backscatter of the ultrasound waves by resonance within sonic windows.<sup>95</sup> This results in a marked amplification of the signals from the blood flow and provides additional information about the microvasculature.<sup>94</sup>

CEUS has been applied to HCC management, including surveillance, diagnosis, CEUS-guided treatment, treatment response evaluation, and follow-up.<sup>96</sup> CEUS is safer and more assessable than CECT or CEMRI for real-time dynamic assessment of vascular perfusion. CEUS with Sonazoid provides an additional Kupffer phase, which is similar to MRI with superparamagnetic iron oxide. HCCs in cirrhotic livers usually do not harbour reticuloendothelial (Kupffer) cells, which differ from normal and cirrhotic liver parenchyma. This leads to a visualised defect in Sonazoid uptake in the postvascular or Kupffer phase.<sup>97-100</sup>

The Japan Society of Hepatology and Asian Pacific Association for the Study of the Liver guidelines have incorporated CEUS with Sonazoid into HCC management. The guidelines allow confirmation of HCC when CEUS shows a hypervascular lesion and / or a defect in the Kupffer phase, even if a lesion does not display the typical arterial hyperenhancement and subsequent washout on either CECT or CEMRI. However, CEUS has been removed from the latest American Association for the Study of Liver Diseases guidelines because of potential false-positive HCC diagnosis in patients with ICC and because Sonazoid is not licensed for use in the liver in the United States.<sup>101</sup> The role of CEUS in differentiation of HCC and ICC remains controversial. On CEUS, compared with HCCs, ICCs enhance to a lesser degree and at a later time after injection, as well as washing out more quickly. In experienced hands, CEUS and CECT are comparably

accurate in diagnosing ICC.<sup>102-105</sup>

## Ultrasound Contrast Agents

The first-generation ultrasound contrast agent, Levovist (Bayer Schering Pharma, Berlin, Germany), consists of air within a shell of galactose microparticles (99.9%) / palmitic acid (0.1%). The lack of stability of the microparticles hampers its commercial use.<sup>95</sup> Second-generation ultrasound contrast agents such as SonoVue, Sonazoid, Definity (Lantheus Medical Imaging, North Billerica [MA], USA), and Optison (GE Healthcare, Princeton, NJ, USA) successfully stabilised microbubbles by replacing air with a more inert and slowly diffusing gas such as sulphur hexafluoride or perfluorobutane. Definity consists of octafluoropropane gas within a lipid shell, and Optison consists of octafluoropropane within an albumin shell. Both are approved for cardiac application only.<sup>95,106</sup> SonoVue consists of sulphur hexafluoride (SF<sub>6</sub>) within a phospholipid shell. SF<sub>6</sub> is an inert molecule that does not interact with any other molecule in the body. After destruction of the microbubble, SF<sub>6</sub> gas is excreted through the lungs only. The shell consists of a monolayer of an amphiphilic phospholipid. The outer side of the shell is in contact with blood and has hydrophilic properties, whereas the inner side has hydrophobic properties and the shell can contain SF<sub>6</sub> gas with stability.<sup>94</sup> As only 7.3% of SonoVue is phagocytosed by Kupffer cells, a parenchyma-specific Kupffer phase cannot be obtained. Repeated injections are required to evaluate the entire liver, and thus its use is not approved in Japan.<sup>107</sup> Sonazoid consists of perfluorobutane within a hydrogenated egg phosphatidylserine shell. In contrast to SonoVue, 99% of Sonazoid is phagocytosed by Kupffer cells and thus can be used to obtain both vascular phase and Kupffer phase images. The entire liver can be evaluated during the Kupffer phase, with microbubbles trapped by the Kupffer cells leading to a homogeneous enhancement in normal functioning liver parenchyma.<sup>95</sup> Lesions lacking functioning Kupffer cells, including small malignant tumours, appear as defects. Currently, Sonazoid has been approved only in Japan and Korea for the evaluation of focal liver lesions.<sup>13</sup>

## Mechanism and Technique

The enhancement patterns of CEUS and CECT or CEMRI are not comparable, as the ultrasound contrast agent is retained only within the blood vessels, whereas CT and MRI contrast agents move into the extracellular space until the concentration is balanced between the

intravascular space and the extracellular space.<sup>108</sup>

The recommended dose of Sonazoid for evaluation of the liver is 0.015 ml/kg. Nonetheless, image quality is maintained at doses lower than the recommendation.<sup>107</sup> For SonoVue, after reconstitution as directed, 1 ml of the resulting dispersion contains 8 µl sulphur hexafluoride in the microbubbles, equivalent to 45 µg. The common single injection volume of dispersion is 2.4 ml, although half-dose and repeat injections may be administered as needed.<sup>13</sup>

Vascularity of focal lesions can be evaluated during the arterial phase (10-20 seconds after injection and lasting 30-45 seconds). The PVP starts at 30-45 seconds and lasts for 2-3 minutes, whereas the late phase starts at 2-3 minutes and lasts for 4-6 minutes. On the PVP or late phase images, the degree of washout between the focal liver lesion and the adjacent liver parenchyma can be compared.<sup>108</sup> Washout is defined as the transition of iso- or hyper-enhancement to hypoenhancement as compared to the adjacent normal liver parenchyma.<sup>109</sup> When using Sonazoid, a Kupffer-phase image can be additionally obtained from 10-15 to 120 minutes after injection.<sup>110,111</sup> The equilibrium phase of CECT or CEMRI does not exist on CEUS, as the ultrasound contrast agent is a pure intravascular contrast agent, and no concentration equilibrium can be achieved.<sup>106</sup>

The mechanical index is defined as the peak rarefactional (or negative) pressure divided by the square root of the ultrasound frequency. At a very low mechanical index, microbubbles stay static and only play a role in the scattering of the ultrasound beam. As the mechanical index increases, microbubbles oscillate at their resonance frequency linearly (<0.2) or nonlinearly (0.2-0.5). When the mechanical index is >0.5, microbubbles oscillate strongly and expand, resulting in disruption of the bubbles. CEUS images can be created from either the signals of the nonlinear oscillation of microbubbles or from microbubble destruction.<sup>94</sup> In first-generation ultrasound contrast agents, a high mechanical index of >0.7 is used, and CEUS images are created using signals from microbubble destruction. As a result, only intermittent scanning can be performed for a few seconds and images are recorded frame by frame. In second-generation ultrasound contrast agents, a low mechanical index of <0.3 is used, and thus continuous, real-time scanning is possible.<sup>112</sup> To detect specific

signals from a small amount of ultrasound contrast agent, the use of the contrast-specific ultrasound mode is essential.<sup>106</sup>

### Safety Considerations

Ultrasound contrast agents are excreted via the lungs only after the destruction of the microbubbles and therefore are not nephrotoxic. They are not iodinated and have no effect on thyroid function. Nonetheless, they can be regarded as foreign materials by the immune system and hypersensitivity reactions may occur.<sup>113</sup> The incidence of severe hypersensitivity reaction is about 0.002% in large-scale abdominal application studies.<sup>114,115</sup> The overall incidence of hypersensitivity reaction of ultrasound contrast agents is less than that of iodinated CT contrast agents and is similar to that of MRI gadolinium chelate contrast agents.<sup>113</sup>

SonoVue is contraindicated in patients with acute coronary syndrome or clinically unstable ischaemic cardiac disease, right-to left shunts, severe pulmonary hypertension, uncontrolled systemic hypertension, and adult respiratory distress syndrome.<sup>116</sup> Sonazoid is contraindicated in patients with right-to-left shunts, severe pulmonary hypertension, and adult respiratory distress syndrome. Sonazoid should be avoided or used with extreme caution in patients with egg allergies, as its shell is made of hydrogenated egg phosphatidylserine sodium. The safety of SonoVue and Sonazoid has not been evaluated in pregnant women; both should be avoided in women who are breast-feeding or in patients younger than 18 years.<sup>13</sup>

Insonation of microbubbles may cause harmful effects to cells or tissue, such as microvascular rupture, haemolysis of red blood cells, increased heating around the ultrasound contrast agent, and killing of phagocytic cells that have engulfed the contrast agent.<sup>115</sup> The European Federation of Societies for Ultrasound in Medicine and Biology recommends use with caution, as damage to the microvessels of the eye or brain can be clinically harmful.<sup>117</sup> A mechanical index of >0.4 rapidly accelerates this harmful biological effect and hence it should be maintained as low as possible.<sup>115</sup>

### Diagnosis of Hepatocellular Carcinoma

On CEUS, 93.5% to 97% of HCCs in cirrhotic livers exhibit arterial hyperenhancement in comparison with the surrounding liver tissue. Hyperenhancement in the arterial phase is usually homogeneous and intense, but may be inhomogeneous in larger nodules (>5 cm),

because of regional necrosis. A thin, perilesional, rim-like hyperenhancement is seen in about 5% to 34.6% of HCCs, which may represent the tumour capsule or blood vessels around the lesion.<sup>118-121</sup> Most HCCs show earlier enhancement than the surrounding liver tissue. The detection rates of hyperenhancement in lesions  $\leq 1.0$  cm, 1.1-2.0 cm, and 2.1-3.0 cm are 67%, 83%-88%, and 92%-100%, respectively. CEUS has a relatively low ability to determine the characteristics of smaller lesions.<sup>120-123</sup>

Washout in the PVP to late phase is characteristic of HCC and is more common in larger lesions (up to 80.4% in PVP and 95.3% in late phase).<sup>118,119</sup> In lesions measuring 1-2 cm, only 53.5% exhibit washout in the PVP and 69% to 90.7% in the late phase.<sup>120,124</sup> Washout is observed more frequently and quickly in HCCs with poorer grades of differentiation, compared with well-differentiated HCCs, which tend to be iso-enhanced in the late phase.<sup>125-127</sup> Compared with other liver malignancies such as ICC and metastatic liver cancer, HCC usually has less marked washout in the late phase.<sup>104,105,128,129</sup> In HCC, washout tends to start later (60 seconds after injection), and in about 25% of cases, washout appears only after 180 seconds. Therefore, it is important to observe nodules in cirrhosis for  $>4$  minutes to increase the sensitivity for the diagnosis of HCC (Figure 6).<sup>128</sup>

Pathologically, large regenerative nodules and low-grade dysplastic nodules generally show arterial and capillary supply similar to that detected in the adjacent cirrhotic nodules, whereas high-grade dysplastic nodules and HCCs may show abnormally increased arterial supply. 33.3% to 60% of high-grade dysplastic nodules show arterial hyperenhancement, whereas 40% to 66.7% show hypo-enhancement. Washout is seldom seen in the late phase for high-grade dysplastic nodules, in contrast to typical HCCs.<sup>122,124</sup>

The sensitivity, specificity, and positive predictive value of CEUS in diagnosing HCC are 88.8%, 89.2%, and 91.3%, respectively.<sup>119</sup> Diagnostic ability is associated with nodule size; sensitivity for nodules of 1.0-2.0 cm, 2.1-3.0 cm, and 3.1-5.0 cm is 69%-80%, 97%, and 100%, respectively, and the specificity is 82%-87%, 97%, and 100%, respectively.<sup>118,120,124</sup>

### Hepatocellular Carcinoma Surveillance

Conventional ultrasonography is non-invasive, low cost, has no radiation exposure, and is easily accessible,

but its diagnostic accuracy is insufficient for HCC, particularly for small lesions.<sup>130</sup>

CEUS is not recommended as the sole imaging tool to screen for HCC, because its arterial phase is too short to examine the entire liver, and washout in the PVP or late phase may not be always detected in small or well-differentiated HCCs.<sup>13</sup>

In CEUS with Sonazoid, HCCs appear hypoechoic on the Kupffer phase, and the entire liver can be assessed with a single injection (Figure 7). Its specificity in diagnosing HCC is higher than that of conventional B-mode ultrasonography (97.8%-98.2% vs. 89.2%-94.9%).<sup>131</sup> The positive and negative predictive values have been reported as 99% and 97%, respectively.<sup>117</sup> Histologically advanced HCC might appear as more hypoechoic than the adjacent liver parenchyma on the Kupffer phase, which is comparable to the signal intensity difference in the HBP of Gd-EOB-DTPA-enhanced MRI.<sup>132</sup> In addition, the defect reperfusion image in both Kupffer-phase and arterial phase images can be evaluated simultaneously and with the same slice by reinjection of Sonazoid during the Kupffer phase.<sup>133</sup> CEUS with Sonazoid has higher diagnostic accuracy (95%) than CECT (82%) in the depiction of malignant hepatic lesions using the defect reperfusion technique.<sup>134</sup>

In patients with compensated hepatitis C virus-related liver cirrhosis, CEUS with Sonazoid is a cost-effective screening tool when the annual incidence of HCC is  $>2\%$  and the sensitivity of CEUS in detecting HCC is  $>80\%$ .<sup>135</sup> Nonetheless, most centres prefer to use CEUS as a problem-solving tool, particularly for nodules measuring 1-2 cm.<sup>136</sup>

### Hepatocellular Carcinoma Intervention

In lesions with atypical patterns, ultrasound-guided percutaneous biopsy is recommended for definitive pathological diagnosis. CEUS prior to biopsy procedures can increase the diagnostic yield by 10% and decrease the false-negative rate, especially in large tumours with areas of necrosis. CEUS can localise the optimal site for biopsy by demonstrating regions of vascularised viable tumours and by avoiding regions of necrosis.<sup>137</sup>

Common HCC treatments include surgical resection and liver transplantation, ethanol ablation, radiofrequency ablation, and microwave ablation, particularly for small or focal recurrent / residual HCC lesions. Survival after

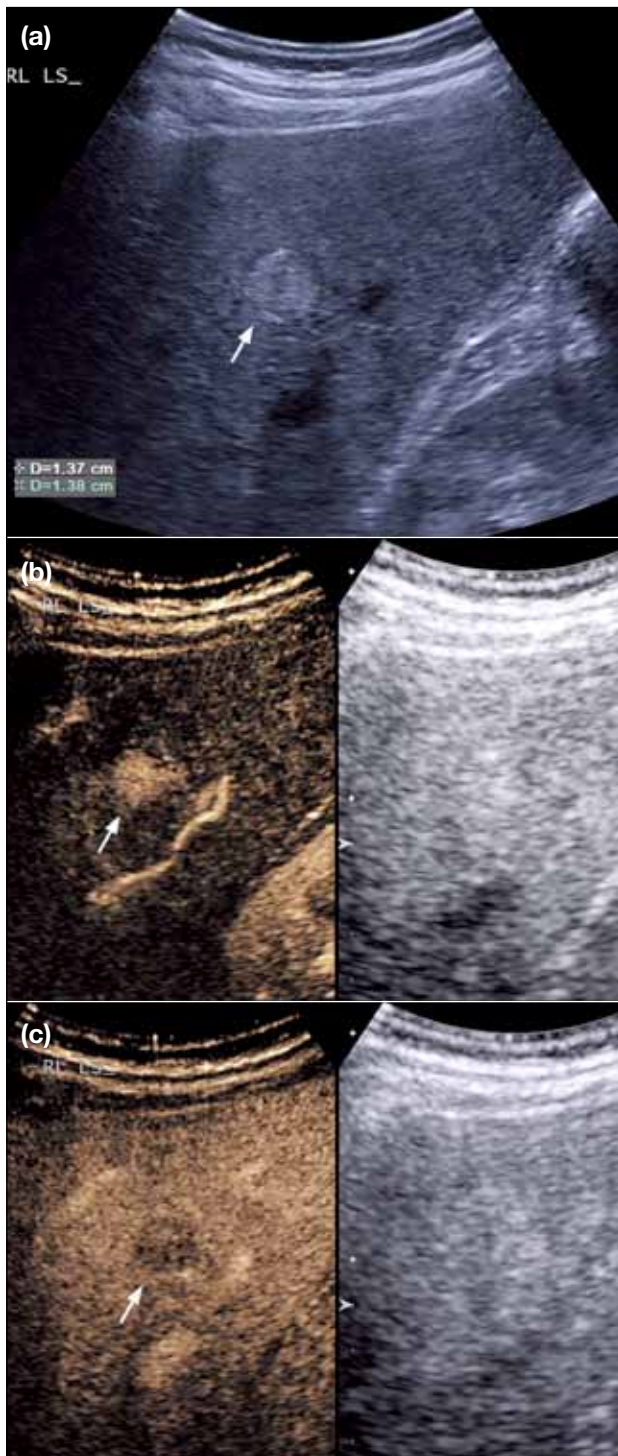


**Figure 6.** (a) Pre-contrast injection ultrasonography of the liver showing a well-defined hyperechoic lesion at segment VI (arrow). Contrast-enhanced ultrasonography with Sonoazoid showing avid homogeneous arterial enhancement of the lesion (b) in the arterial phase, and contrast washout (c) in the portovenous phase indicating a hepatocellular carcinoma (arrows).

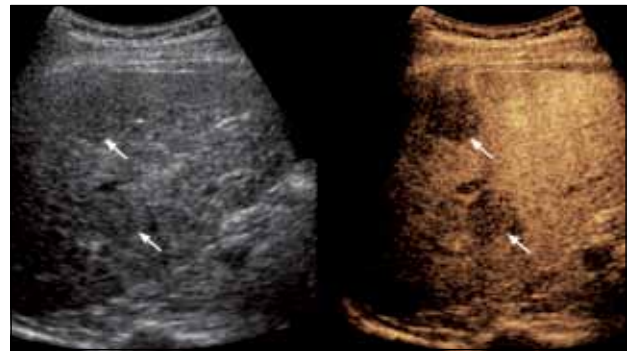


**Figure 7.** Conventional ultrasonography of the liver showing two isoechoic lesions (arrows) that are distinctly hypoechoic (arrows) in the Kupffer phase on contrast-enhanced ultrasonography with Sonoazoid (Courtesy of Prof. MJ Kim, Department of Radiology, Yonsei University College of Medicine).

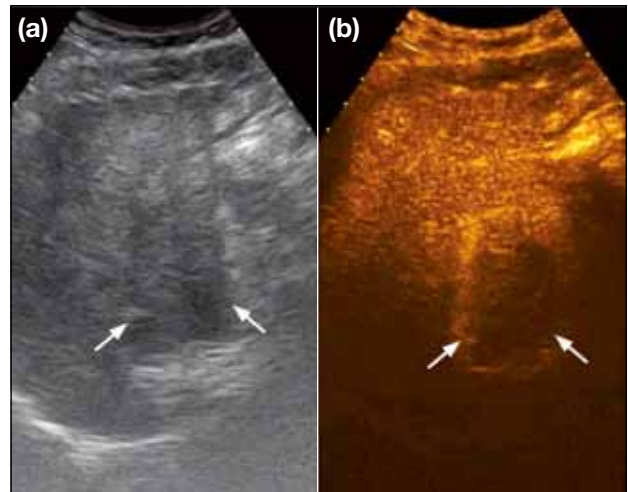


**Figure 8.** Immediately after radiofrequency ablation for a hepatocellular carcinoma, the ablative zone (arrows) is hypoechoic on (a) conventional ultrasonography and has a thin rim enhancement on (b) contrast-enhanced ultrasonography with SonoVue, indicating post-ablative hyperaemia.

ablation in Child-Pugh A patients is 50% to 70% at 5 years, comparable to that after resection.<sup>138-140</sup> Prior to percutaneous therapy, CEUS can be used to assess HCC lesion size, margins, and its relationship with the surrounding structures, and to plan the treatment strategy.<sup>128</sup> CEUS can also guide the real-time puncture during the arterial phase, PVP, late phase and in the instance of Sonoazoid contrast, the Kupffer phase. For multiple lesions, ultrasound contrast agents can be

administered repeatedly to guide percutaneous therapy at multiple sites.<sup>128,141</sup>

Fusion imaging with conventional ultrasonography and CECT or CEMRI can be used for guiding biopsy or ablation of inconspicuous lesions. About 83% of HCCs that are inconspicuous on fusion imaging with conventional ultrasonography are well visualised on CEUS.<sup>142</sup>

### Treatment Response

The use of CECT or CEMRI to detect residual viable tumour or recurrent HCC for treatment response evaluation is widely accepted.<sup>143,144</sup> CEUS is regarded as a competent alternative for this purpose.<sup>143,145-151</sup>

Intra-procedural CEUS is effective and comparable to early follow-up CECT in the assessment of percutaneous ablative therapies and adequacy of ablative margins.<sup>145,148,152,153</sup> Intra-procedural CEUS reduces the numbers of incomplete treatments and re-treatments and the total cost of radiofrequency ablation for HCC.<sup>152</sup> Nonetheless, post-procedural reactive hyperaemia commences soon after ablative therapy, lasting up to a few weeks, potentially obscuring small-volume residual viable tumour. Uniform rim enhancement can be seen up to 30 days after radiofrequency ablation and should not be misdiagnosed as marginal tumour recurrence (Figure 8).<sup>106</sup>

The role of CEUS versus CECT or MRI for long-term surveillance remains controversial.<sup>153</sup> According to the modified Response Evaluation Criteria in Solid Tumors, viable HCC is defined as uptake of contrast agent in the arterial phase of CEUS, whereas complete response is defined as disappearance of any intratumoural arterial enhancement in HCC.<sup>149</sup> CEUS and CECT show conflicting results depending on the timing of follow-up; their results are comparable at 1 month or earlier, although the sensitivity of CEUS in detecting both local recurrence and new intrahepatic recurrence in long-term follow-up is lower than that of CECT.<sup>154</sup> For response evaluation after transarterial chemoembolisation, the accuracy of CEUS ranges from 72.6% to 100% and that of CECT from 61% to 94%.<sup>143</sup> The suboptimal performance of CEUS in long-term follow-up can be attributed to its difficulty in providing an overview of the entire liver to detect HCC progression and intrahepatic recurrence even after reinjection of contrast.<sup>128,153,154</sup> Nonetheless, when CECT or CEMRI is contraindicated or inconclusive, CEUS may be an

alternative to assess tumour progression and intrahepatic recurrence.<sup>106,128</sup>

### Guidelines on Management of Hepatocellular Carcinoma

Most guidelines recommend multiphase multidetector row CT and / or contrast-enhanced ECA-MRI as the standard imaging modalities for diagnosis of HCC, based on the typical arterial phase hyperenhancement and washout on the PVP or delayed phase. Gd-EOB-MRI is recommended as the primary diagnostic imaging modality for the diagnosis of HCC by the Japan Society of Hepatology, the Korean Liver Cancer Study Group and National Cancer Center, and the LI-RADS, which is acknowledged by the American Association for the Study of Liver Diseases.<sup>18</sup> The guidelines set by the European Association for the Study of the Liver-European Organisation for Research and Treatment of Cancer and the Asian Pacific Association for the Study of the Liver are being updated.

According to the 2014 Japan Society of Hepatology guidelines, a non-invasive diagnosis of HCC can be made when a mass shows: (1) arterial hypervascularity and venous washout, (2) arterial hypervascularity without venous washout but with hypointensity on the HBP, or (3) arterial hypovascularity on Gd-EOB-MRI but with hypervascularity on CEUS with Sonazoid and / or defect in the Kupffer phase. Haemangioma must be excluded; it can exhibit pseudowashout in the transition phase (the late dynamic phase between PVP and HBP usually in a 3-minute delayed scan), and hypointensity on the HBP as well as defect in the Kupffer phase on CEUS with Sonazoid.<sup>18</sup>

According to the 2014 Korean Liver Cancer Study Group and National Cancer Center guidelines, hypointensity on the HBP cannot be regarded as an alternative to washout, but hypoenhancement on the 3-minute delayed scan can be considered as washout.<sup>18</sup>

In contrast, the LI-RADS versions 2014 and 2017 stipulate that washout appearance should only be described on the PVP, as hypointensity on the transition phase alone is partially attributed to the progressive contrast uptake of the background liver parenchyma. It incorporates hypointensity on the HBP as one of the ancillary features of malignancy, thus allowing the observation to be upgraded to LR-4, or probably HCC.<sup>12</sup>

The difference in adoption of Gd-EOB-MRI into

various guidelines reflects the preference of either high sensitivity or high specificity. For example, when hypointensity in the transition phase and / or HBP is considered as an alternative to washout, the sensitivity is increased at the cost of increasing the likelihood of false positive, such as haemangioma and ICC. In countries where liver transplantation is not a prevalent treatment for HCC, the potential increase in false positive and treatment thereof may be considered acceptable.

Compared with Gd-EOB-MRI, CEUS is not well-accepted in management guidelines worldwide. This can be attributed to the limited availability of Sonazoid and hence its user experience.

CEUS and Gd-EOB-MRI are complementary in HCC management. In Hong Kong, both modalities tend to be reserved as problem-solving tools. CEUS with Sonazoid can be a cost-effective strategy in HCC surveillance, and Gd-EOB-MRI is more cost-effective than ECA-MRI and CECT in HCC diagnosis. In addition, CEUS is complementary to conventional ultrasonography during interventional procedures. The use of Gd-EOB-MRI and CEUS in HCC management should be prospectively validated, based on differences in disease incidence, healthcare system, and cost worldwide.

## CONCLUSION

Gd-EOB-MRI improves the ability to detect dysplastic nodules, diagnose early or atypical HCCs, differentiate HCC from vascular pseudolesions and non-hepatocellular tumours, and predict outcome. It is superior to CECT and ECA-MRI and has been included in various HCC management guidelines. CEUS can play a role in HCC surveillance, problem solving in HCC diagnosis, guide interventional procedures, and assess treatment response. Sonazoid has an additional benefit of providing the Kupffer phase, during which the entire liver can be assessed from a single injection.

## REFERENCES

- European Association For The Study Of The Liver; European Organisation For Research And Treatment Of Cancer. EASL-EORTC clinical practice guidelines: management of hepatocellular carcinoma. *J Hepatol.* 2012;56:908-43. [cross ref](#)
- Llovet JM, Fuster J, Bruix J. Intention-to-treat analysis of surgical treatment for early hepatocellular carcinoma: resection versus transplantation. *Hepatology.* 1999;30:1434-40. [cross ref](#)
- Parkin DM, Bray F, Ferlay J, Pisani P. Global cancer statistics, 2002. *CA Cancer J Clin.* 2005;55:74-108. [cross ref](#)
- Kondo Y, Kimura O, Shimosegawa T. Significant biomarkers for the management of hepatocellular carcinoma. *Clin J Gastroenterol.* 2015;8:109-15. [cross ref](#)
- Beasley RP, Hwang LY, Lin CC, Chien CS. Hepatocellular carcinoma and hepatitis B virus. A prospective study of 22 707 men in Taiwan. *Lancet.* 1981;2:1129-33. [cross ref](#)
- Degos F, Christidis C, Ganne-Carrie N, Farmachidi JP, Degott C, Guettier C, et al. Hepatitis C virus related cirrhosis: time to occurrence of hepatocellular carcinoma and death. *Gut.* 2000;47:131-6. [cross ref](#)
- Bruix J, Sherman M, Llovet JM, Beaugrand M, Lencioni R, Burroughs AK, et al. Clinical management of hepatocellular carcinoma. Conclusions of the Barcelona-2000 EASL conference. European Association for the Study of the Liver. *J Hepatol.* 2001;35:421-30. [cross ref](#)
- Bota S, Piscaglia F, Marinelli S, Pecorelli A, Terzi E, Bolondi L. Comparison of international guidelines for noninvasive diagnosis of hepatocellular carcinoma. *Liver Cancer.* 2012;1:190-200. [cross ref](#)
- Kudo M, Matsui O, Izumi N, Iijima H, Kadoya M, Imai Y, et al. Surveillance and diagnostic algorithm for hepatocellular carcinoma proposed by the Liver Cancer Study Group of Japan: 2014 update. *Oncology.* 2014;87(Suppl 1):7-21. [cross ref](#)
- Lee JM, Park JW, Choi BI. 2014 KLCSCG-NCC Korea Practice Guidelines for the management of hepatocellular carcinoma: HCC diagnostic algorithm. *Dig Dis.* 2014;32:764-77. [cross ref](#)
- Mitchell DG, Bruix J, Sherman M, Sirlin CB. LI-RADS (Liver Imaging Reporting and Data System): summary, discussion, and consensus of the LI-RADS Management Working Group and future directions. *Hepatology.* 2015;61:1056-65. [cross ref](#)
- Hope TA, Fowler KJ, Sirlin CB, Costa EA, Yee J, Yeh BM, et al. Hepatobiliary agents and their role in LI-RADS. *Abdom Imaging.* 2015;40:613-25. [cross ref](#)
- Chung YE, Kim KW. Contrast-enhanced ultrasonography: advance and current status in abdominal imaging. *Ultrasonography.* 2015;34:3-18. [cross ref](#)
- Kudo M. Will Gd-EOB-MRI change the diagnostic algorithm in hepatocellular carcinoma? *Oncology.* 2010;78(Suppl 1):87-93. [cross ref](#)
- Schraml C, Kaufmann S, Rempp H, Syha R, Ketelsen D, Notohamiprodjo M, et al. Imaging of HCC: current state of the art. *Diagnostics (Basel).* 2015;5:513-45. [cross ref](#)
- de Lope CR, Tremosini S, Forner A, Reig M, Bruix J. Management of HCC. *J Hepatol.* 2012;56(Suppl 1):S75-87. [cross ref](#)
- Bargellini I, Battaglia V, Bozzi E, Lauretti DL, Lorenzoni G, Bartolozzi C. Radiological diagnosis of hepatocellular carcinoma. *J Hepatocell Carcinoma.* 2014;1:137-48. [cross ref](#)
- Joo I, Lee JM. Recent advances in the imaging diagnosis of hepatocellular carcinoma: value of Gadoxetic acid-enhanced MRI. *Liver Cancer.* 2016;5:67-87. [cross ref](#)
- Van Beers BE, Pastor CM, Hussain HK. Primovist, Eovist: what to expect? *J Hepatol.* 2012;57:421-9. [cross ref](#)
- Seale MK, Catalano OA, Saini S, Hahn PF, Sahani DV. Hepatobiliary-specific MR contrast agents: role in imaging the liver and biliary tree. *Radiographics.* 2009;29:1725-48. [cross ref](#)
- Tanimoto A, Kadoya M, Kawamura Y, Kuwatsuru R, Gokan T, Hirohashi S. Safety and efficacy of a novel hepatobiliary MR contrast agent, Gd-DTPA-DeA: results of phase I and phase II clinical trials. *J Magn Reson Imaging.* 2006;23:499-508. [cross ref](#)
- Tamada T, Ito K, Sone T, Yamamoto A, Yoshida K, Kakuba K, et al. Dynamic contrast-enhanced magnetic resonance imaging of abdominal solid organ and major vessel: comparison of enhancement effect between Gd-EOB-DTPA and Gd-DTPA. *J Magn Reson Imaging.* 2009;29:636-40. [cross ref](#)
- Tanimoto A, Lee JM, Murakami T, Huppertz A, Kudo M, Grazioli L. Consensus report of the 2nd International Forum for Liver MRI. *Eur Radiol.* 2009;19(Suppl 5):S975-89. [cross ref](#)
- Motosugi U, Ichikawa T, Tominaga L, Sou H, Sano K, Ichikawa

- S, et al. Delay before the hepatocyte phase of Gd-EOB-DTPA-enhanced MR imaging: is it possible to shorten the examination time? *Eur Radiol.* 2009;19:2623-9. [crossref](#)
25. Bluemke DA, Sahani D, Amendola M, Balzer T, Breuer J, Brown JJ, et al. Efficacy and safety of MR imaging with liver-specific contrast agent: U.S. multicenter phase III study. *Radiology.* 2005;237:89-98. [crossref](#)
  26. Willatt JM, Hussain HK, Adusumilli S, Marrero JA. MR Imaging of hepatocellular carcinoma in the cirrhotic liver: challenges and controversies. *Radiology.* 2008;247:311-30. [crossref](#)
  27. Lee JM, Choi BI. Hepatocellular nodules in liver cirrhosis: MR evaluation. *Abdom Imaging.* 2011;36:282-9. [crossref](#)
  28. The International Consensus Group for Hepatocellular Neoplasia. Pathologic diagnosis of early hepatocellular carcinoma: a report of The International Consensus Group for Hepatocellular Neoplasia. *Hepatology.* 2009;49:658-64. [crossref](#)
  29. Roskams T, Kojiro M. Pathology of early hepatocellular carcinoma: conventional and molecular diagnosis. *Semin Liver Dis.* 2010;30:17-25. [crossref](#)
  30. Kim HD, Lim YS, Han S, An J, Kim GA, Kim SY, et al. Evaluation of early-stage hepatocellular carcinoma by magnetic resonance imaging with gadoxetic acid detects additional lesions and increases overall survival. *Gastroenterology.* 2015;148:1371-82. [crossref](#)
  31. Park MJ, Kim YK, Lee MW, Lee WJ, Kim YS, Kim SH, et al. Small hepatocellular carcinomas: improved sensitivity by combining gadoxetic acid-enhanced and diffusion-weighted MR imaging patterns. *Radiology.* 2012;264:761-70. [crossref](#)
  32. Park MJ, Kim YK, Lee MH, Lee JH. Validation of diagnostic criteria using gadoxetic acid-enhanced and diffusion-weighted MR imaging for small hepatocellular carcinoma ( $\leq 2.0$  cm) in patients with hepatitis-induced liver cirrhosis. *Acta Radiol.* 2013;54:127-36. [crossref](#)
  33. Choi JY, Lee JM, Sirlin CB. CT and MR imaging diagnosis and staging of hepatocellular carcinoma: part I. Development, growth, and spread: key pathologic and imaging aspects. *Radiology.* 2014;272:635-54. [crossref](#)
  34. Ichikawa T, Sano K, Morisaka H. Diagnosis of pathologically early HCC with EOB-MRI: experiences and current consensus. *Liver Cancer.* 2014;3:97-107. [crossref](#)
  35. Chou CT, Chen YL, Su WW, Wu HK, Chen RC. Characterization of cirrhotic nodules with gadoxetic acid-enhanced magnetic resonance imaging: the efficacy of hepatocyte-phase imaging. *J Magn Reson Imaging.* 2010;32:895-902. [crossref](#)
  36. Inchingolo R, De Gaetano AM, Curione D, Ciresa M, Miele L, Pompili M, et al. Role of diffusion-weighted imaging, apparent diffusion coefficient and correlation with hepatobiliary phase findings in the differentiation of hepatocellular carcinoma from dysplastic nodules in cirrhotic liver. *Eur Radiol.* 2015;25:1087-96. [crossref](#)
  37. Narita M, Hatano E, Arizono S, Miyagawa-Hayashino A, Isoda H, Kitamura K, et al. Expression of OATP1B3 determines uptake of Gd-EOB-DTPA in hepatocellular carcinoma. *J Gastroenterol.* 2009;44:793-8. [crossref](#)
  38. Kitao A, Zen Y, Matsui O, Gabata T, Kobayashi S, Koda W, et al. Hepatocellular carcinoma: signal intensity at gadoxetic acid-enhanced MR imaging—correlation with molecular transporters and histopathologic features. *Radiology.* 2010;256:817-26. [crossref](#)
  39. Suh YJ, Kim MJ, Choi JY, Park YN, Park MS, Kim KW. Differentiation of hepatic hyperintense lesions seen on gadoxetic acid-enhanced hepatobiliary phase MRI. *AJR Am J Roentgenol.* 2011;197:W44-52. [crossref](#)
  40. Bookstein JJ, Cho KJ, Davis GB, Dail D. Arteriportal communications: observations and hypotheses concerning transsinusoidal and transvasal types. *Radiology.* 1982;142:581-90. [crossref](#)
  41. Ahn JH, Yu JS, Hwang SH, Chung JJ, Kim JH, Kim KW. Nontumorous arteriportal shunts in the liver: CT and MRI findings considering mechanisms and fate. *Eur Radiol.* 2010;20:385-94. [crossref](#)
  42. Motosugi U, Ichikawa T, Sou H, Sano K, Tominaga L, Muhi A, et al. Distinguishing hypervascular pseudolesions of the liver from hypervascular hepatocellular carcinomas with gadoxetic acid-enhanced MR imaging. *Radiology.* 2010;256:151-8. [crossref](#)
  43. Zhou XD, Tang ZY, Fan J, Zhou J, Wu ZQ, Qin LX, et al. Intrahepatic cholangiocarcinoma: report of 272 patients compared with 5,829 patients with hepatocellular carcinoma. *J Cancer Res Clin Oncol.* 2009;135:1073-80. [crossref](#)
  44. Lee JH, Chung GE, Yu SJ, Hwang SY, Kim JS, Kim HY, et al. Long-term prognosis of combined hepatocellular and cholangiocarcinoma after curative resection comparison with hepatocellular carcinoma and cholangiocarcinoma. *J Clin Gastroenterol.* 2011;45:69-75.
  45. Zhang Y, Uchida M, Abe T, Nishimura H, Hayabuchi N, Nakashima Y. Intrahepatic peripheral cholangiocarcinoma: comparison of dynamic CT and dynamic MRI. *J Comput Assist Tomogr.* 1999;23:670-7. [crossref](#)
  46. Rimola J, Forner A, Reig M, Vilana R, de Lope CR, Ayuso C, et al. Cholangiocarcinoma in cirrhosis: absence of contrast washout in delayed phases by magnetic resonance imaging avoids misdiagnosis of hepatocellular carcinoma. *Hepatology.* 2009;50:791-8. [crossref](#)
  47. Kim SJ, Lee JM, Han JK, Kim KH, Lee JY, Choi BI. Peripheral mass-forming cholangiocarcinoma in cirrhotic liver. *AJR Am J Roentgenol.* 2007;189:1428-34. [crossref](#)
  48. Xu J, Igarashi S, Sasaki M, Matsubara T, Yoneda N, Kozaka K, et al. Intrahepatic cholangiocarcinomas in cirrhosis are hypervascular in comparison with those in normal livers. *Liver Int.* 2012;32:1156-64. [crossref](#)
  49. Kang Y, Lee JM, Kim SH, Han JK, Choi BI. Intrahepatic mass-forming cholangiocarcinoma: enhancement patterns on gadoxetic acid-enhanced MR images. *Radiology.* 2012;264:751-60. [crossref](#)
  50. Asayama Y, Nishie A, Ishigami K, Ushijima Y, Takayama Y, Fujita N, et al. Distinguishing intrahepatic cholangiocarcinoma from poorly differentiated hepatocellular carcinoma using precontrast and gadoxetic acid-enhanced MRI. *Diagn Interv Radiol.* 2015;21:96-104. [crossref](#)
  51. Park MJ, Kim YK, Park HJ, Hwang J, Lee WJ. Scirrhous hepatocellular carcinoma on gadoxetic acid-enhanced magnetic resonance imaging and diffusion-weighted imaging: emphasis on the differentiation of intrahepatic cholangiocarcinoma. *J Comput Assist Tomogr.* 2013;37:872-81. [crossref](#)
  52. Chong YS, Kim YK, Lee MW, Kim SH, Lee WJ, Rhim HC, et al. Differentiating mass-forming intrahepatic cholangiocarcinoma from atypical hepatocellular carcinoma using gadoxetic acid-enhanced MRI. *Clin Radiol.* 2012;67:766-73. [crossref](#)
  53. Kanematsu M, Kondo H, Goshima S, Kato H, Tsuge U, Hirose Y, et al. Imaging liver metastases: review and update. *Eur J Radiol.* 2006;58:217-28. [crossref](#)
  54. Park YS, Lee CH, Kim JW, Shin S, Park CM. Differentiation of hepatocellular carcinoma from its various mimickers in liver magnetic resonance imaging: what are the tips when using hepatocyte-specific agents? *World J Gastroenterol.* 2016;22:284-99. [crossref](#)
  55. Tamada T, Ito K, Yamamoto A, Sone T, Kanki A, Tanaka F, et al. Hepatic hemangiomas: evaluation of enhancement patterns at dynamic MRI with gadoxetate disodium. *AJR Am J Roentgenol.*

- 2011;196:824-30. [crossref](#)
56. Doo KW, Lee CH, Choi JW, Lee J, Kim KA, Park CM. "Pseudo washout" sign in high-flow hepatic hemangioma on gadoxetic acid contrast-enhanced MRI mimicking hypervascular tumor. *AJR Am J Roentgenol.* 2009;193:W490-6. [crossref](#)
  57. Nam SJ, Park KY, Yu JS, Chung JJ, Kim JH, Kim KW. Hepatic cavernous hemangiomas: relationship between speed of intratumoral enhancement during dynamic MRI and apparent diffusion coefficient on diffusion-weighted imaging. *Korean J Radiol.* 2012;13:728-35. [crossref](#)
  58. Nonomura A, Enomoto Y, Takeda M, Takano M, Morita K, Kasai T. Angiomyolipoma of the liver: a reappraisal of morphological features and delineation of new characteristic histological features from the clinicopathological findings of 55 tumours in 47 patients. *Histopathology.* 2012;61:863-80. [crossref](#)
  59. Wang SY, Kuai XP, Meng XX, Jia NY, Dong H. Comparison of MRI features for the differentiation of hepatic angiomyolipoma from fat-containing hepatocellular carcinoma. *Abdom Imaging.* 2014;39:323-33. [crossref](#)
  60. Cai PQ, Wu YP, Xie CM, Zhang WD, Han R, Wu PH. Hepatic angiomyolipoma: CT and MR imaging findings with clinical-pathologic comparison. *Abdom Imaging.* 2013;38:482-9. [crossref](#)
  61. Kim R, Lee JM, Joo I, Lee DH, Woo S, Han JK, et al. Differentiation of lipid poor angiomyolipoma from hepatocellular carcinoma on gadoxetic acid-enhanced liver MR imaging. *Abdom Imaging.* 2015;40:531-41. [crossref](#)
  62. Hanna RF, Miloushev VZ, Tang A, Finklestone LA, Brejt SZ, Sandhu RS, et al. Comparative 13-year meta-analysis of the sensitivity and positive predictive value of ultrasound, CT, and MRI for detecting hepatocellular carcinoma. *Abdom Radiol (NY).* 2016;41:71-90. [crossref](#)
  63. Ooka Y, Kanai F, Okabe S, Ueda T, Shimofusa R, Ogasawara S, et al. Gadoxetic acid-enhanced MRI compared with CT during angiography in the diagnosis of hepatocellular carcinoma. *Magn Reson Imaging.* 2013;31:748-54. [crossref](#)
  64. Park G, Kim YK, Kim CS, Yu HC, Hwang SB. Diagnostic efficacy of gadoxetic acid-enhanced MRI in the detection of hepatocellular carcinomas: comparison with gadopentetate dimeglumine. *Br J Radiol.* 2010;83:1010-6. [crossref](#)
  65. Frericks BB, Loddenkemper C, Huppertz A, Valdeig S, Stroux A, Seja M, et al. Qualitative and quantitative evaluation of hepatocellular carcinoma and cirrhotic liver enhancement using Gd-EOB-DTPA. *AJR Am J Roentgenol.* 2009;193:1053-60. [crossref](#)
  66. Kim HS, Choi D, Kim SH, Lee MW, Lee WJ, Kim YK, et al. Changes in the signal- and contrast-to-noise ratios of hepatocellular carcinomas on gadoxetic acid-enhanced dynamic MR imaging. *Eur J Radiol.* 2013;82:62-8. [crossref](#)
  67. Sano K, Ichikawa T, Motosugi U, Sou H, Muhi AM, Matsuda M, et al. Imaging study of early hepatocellular carcinoma: usefulness of gadoxetic acid-enhanced MR imaging. *Radiology.* 2011;261:834-44. [crossref](#)
  68. Ahn SS, Kim MJ, Lim JS, Hong HS, Chung YE, Choi JY. Added value of gadoxetic acid-enhanced hepatobiliary phase MR imaging in the diagnosis of hepatocellular carcinoma. *Radiology.* 2010;255:459-66. [crossref](#)
  69. Golfieri R, Grazioli L, Orlando E, Dormi A, Lucidi V, Corcioni B, et al. Which is the best MRI marker of malignancy for atypical cirrhotic nodules: hypointensity in hepatobiliary phase alone or combined with other features? Classification after Gd-EOB-DTPA administration. *J Magn Reson Imaging.* 2012;36:648-57. [crossref](#)
  70. Granito A, Galassi M, Piscaglia F, Romanini L, Lucidi V, Renzulli M, et al. Impact of gadoxetic acid (Gd-EOB-DTPA)-enhanced magnetic resonance on the non-invasive diagnosis of small hepatocellular carcinoma: a prospective study. *Aliment Pharmacol Ther.* 2013;37:355-63. [crossref](#)
  71. Haradome H, Grazioli L, Tinti R, Morone M, Motosugi U, Sano K, et al. Additional value of gadoxetic acid-DTPA-enhanced hepatobiliary phase MR imaging in the diagnosis of early-stage hepatocellular carcinoma: comparison with dynamic triple-phase multidetector CT imaging. *J Magn Reson Imaging.* 2011;34:69-78. [crossref](#)
  72. Onishi H, Kim T, Imai Y, Hori M, Nagano H, Nakaya Y, et al. Hypervascular hepatocellular carcinomas: detection with gadoxetate disodium-enhanced MR imaging and multiphasic multidetector CT. *Eur Radiol.* 2012;22:845-54. [crossref](#)
  73. Bashir MR, Gupta RT, Davenport MS, Allen BC, Jaffe TA, Ho LM, et al. Hepatocellular carcinoma in a North American population: does hepatobiliary MR imaging with Gd-EOB-DTPA improve sensitivity and confidence for diagnosis? *J Magn Reson Imaging.* 2013;37:398-406. [crossref](#)
  74. Chou CT, Chen YL, Wu HK, Chen RC. Characterization of hyperintense nodules on precontrast T1-weighted MRI: utility of gadoxetic acid-enhanced hepatocyte-phase imaging. *J Magn Reson Imaging.* 2011;33:625-32. [crossref](#)
  75. Nishie A, Goshima S, Haradome H, Hatano E, Imai Y, Kudo M, et al. Cost-effectiveness of EOB-MRI for hepatocellular carcinoma in Japan. *Clin Ther.* 2017;39:738-50. [crossref](#)
  76. Kim HY, Choi JY, Kim CW, Bae SH, Yoon SK, Lee YJ, et al. Gadolinium ethoxybenzyl diethylenetriamine pentaacetic acid-enhanced magnetic resonance imaging predicts the histological grade of hepatocellular carcinoma only in patients with Child-Pugh class A cirrhosis. *Liver Transpl.* 2012;18:850-7. [crossref](#)
  77. Kitao A, Matsui O, Yoneda N, Kozaka K, Shinmura R, Koda W, et al. The uptake transporter OATP8 expression decreases during multistep hepatocarcinogenesis: correlation with gadoxetic acid enhanced MR imaging. *Eur Radiol.* 2011;21:2056-66. [crossref](#)
  78. Kogita S, Imai Y, Okada M, Kim T, Onishi H, Takamura M, et al. Gd-EOB-DTPA-enhanced magnetic resonance images of hepatocellular carcinoma: correlation with histological grading and portal blood flow. *Eur Radiol.* 2010;20:2405-13. [crossref](#)
  79. Saito K, Moriyasu F, Sugimoto K, Nishio R, Saguchi T, Nagao T, et al. Diagnostic efficacy of gadoxetic acid-enhanced MRI for hepatocellular carcinoma and dysplastic nodule. *World J Gastroenterol.* 2011;17:3503-9. [crossref](#)
  80. Sugimoto K, Moriyasu F, Saito K, Taira J, Saguchi T, Yoshimura N, et al. Comparison of Kupffer-phase Sonazoid-enhanced sonography and hepatobiliary-phase gadoxetic acid-enhanced magnetic resonance imaging of hepatocellular carcinoma and correlation with histologic grading. *J Ultrasound Med.* 2012;31:529-38. [crossref](#)
  81. Choi JW, Lee JM, Kim SJ, Yoon JH, Baek JH, Han JK, et al. Hepatocellular carcinoma: imaging patterns on gadoxetic acid-enhanced MR Images and their value as an imaging biomarker. *Radiology.* 2013;267:776-86. [crossref](#)
  82. Kim JY, Kim MJ, Kim KA, Jeong HT, Park YN. Hyperintense HCC on hepatobiliary phase images of gadoxetic acid-enhanced MRI: correlation with clinical and pathological features. *Eur J Radiol.* 2012;81:3877-82. [crossref](#)
  83. Kitao A, Matsui O, Yoneda N, Kozaka K, Kobayashi S, Koda W, et al. Hypervascular hepatocellular carcinoma: correlation between biologic features and signal intensity on gadoxetic acid-enhanced MR images. *Radiology.* 2012;265:780-9. [crossref](#)
  84. Jeong HT, Kim MJ, Kim YE, Park YN, Choi GH, Choi JS. MRI features of hepatocellular carcinoma expressing progenitor cell markers. *Liver Int.* 2012;32:430-40.
  85. Ariizumi S, Kitagawa K, Kotera Y, Takahashi Y, Katagiri

- S, Kuwatsuru R, et al. A non-smooth tumor margin in the hepatobiliary phase of gadoxetic acid disodium (Gd-EOB-DTPA)-enhanced magnetic resonance imaging predicts microscopic portal vein invasion, intrahepatic metastasis, and early recurrence after hepatectomy in patients with hepatocellular carcinoma. *J Hepatobiliary Pancreat Sci.* 2011;18:575-85. [crossref](#)
86. Fujita N, Nishie A, Kubo Y, Asayama Y, Ushijima Y, Takayama Y, et al. Hepatocellular carcinoma: clinical significance of signal heterogeneity in the hepatobiliary phase of gadoxetic acid-enhanced MR imaging. *Eur Radiol.* 2015;25:211-20. [crossref](#)
  87. Akai H, Matsuda I, Kiryu S, Tajima T, Takao H, Watanabe Y, et al. Fate of hypointense lesions on Gd-EOB-DTPA-enhanced magnetic resonance imaging. *Eur J Radiol.* 2012;81:2973-7. [crossref](#)
  88. Hyodo T, Murakami T, Imai Y, Okada M, Hori M, Kagawa Y, et al. Hypovascular nodules in patients with chronic liver disease: risk factors for development of hypervascular hepatocellular carcinoma. *Radiology.* 2013;266:480-90. [crossref](#)
  89. Kobayashi S, Matsui O, Gabata T, Koda W, Minami T, Ryu Y, et al. Gadolinium ethoxybenzyl diethylenetriamine pentaacetic acid-enhanced magnetic resonance imaging findings of borderline lesions at high risk for progression to hypervascular classic hepatocellular carcinoma. *J Comput Assist Tomogr.* 2011;35:181-6. [crossref](#)
  90. Kumada T, Toyoda H, Tada T, Sone Y, Fujimori M, Ogawa S, et al. Evolution of hypointense hepatocellular nodules observed only in the hepatobiliary phase of gadoxetic acid disodium-enhanced MRI. *AJR Am J Roentgenol.* 2011;197:58-63. [crossref](#)
  91. Motosugi U, Ichikawa T, Sano K, Sou H, Onohara K, Muhi A, et al. Outcome of hypovascular hepatic nodules revealing no gadoxetic acid uptake in patients with chronic liver disease. *J Magn Reson Imaging.* 2011;34:88-94. [crossref](#)
  92. Takechi M, Tsuda T, Yoshioka S, Murata S, Tanaka H, Hirooka M, et al. Risk of hypervascularization in small hypovascular hepatic nodules showing hypointense in the hepatobiliary phase of gadoxetic acid-enhanced MRI in patients with chronic liver disease. *Jpn J Radiol.* 2012;30:743-51. [crossref](#)
  93. Toyoda H, Kumada T, Tada T, Sone Y, Maeda A, Kaneoka Y. Non-hypervascular hypointense nodules on Gd-EOB-DTPA-enhanced MRI as a predictor of outcomes for early-stage HCC. *Hepatol Int.* 2015;9:84-92. [crossref](#)
  94. Greis C. Technology overview: SonoVue (Bracco, Milan). *Eur Radiol.* 2004;14(Suppl 8):P11-5. [crossref](#)
  95. Sontum PC. Physicochemical characteristics of Sonazoid, a new contrast agent for ultrasound imaging. *Ultrasound Med Biol.* 2008;34:824-33. [crossref](#)
  96. Bauer A, Hauff P, Lazenby J, von Behren P, Zomack M, Reinhardt M, et al. Wideband harmonic imaging: a novel contrast ultrasound imaging technique. *Eur Radiol.* 1999;9(Suppl 3):S364-7. [crossref](#)
  97. Hatanaka K, Kudo M, Minami Y, Ueda T, Tatsumi C, Kitai S, et al. Differential diagnosis of hepatic tumors: value of contrast-enhanced harmonic sonography using the newly developed contrast agent, Sonazoid. *Intervirology.* 2008;51(Suppl 1):61-9. [crossref](#)
  98. Inoue T, Kudo M, Hatanaka K, Takahashi S, Kitai S, Ueda T, et al. Imaging of hepatocellular carcinoma: qualitative and quantitative analysis of postvascular phase contrast-enhanced ultrasonography with Sonazoid. Comparison with superparamagnetic iron oxide magnetic resonance images. *Oncology.* 2008;75(Suppl 1):48-54. [crossref](#)
  99. Kudo M, Hatanaka K, Kumada T, Toyoda H, Tada T. Double-contrast ultrasound: a novel surveillance tool for hepatocellular carcinoma. *Am J Gastroenterol.* 2011;106:368-70. [crossref](#)
  100. Moriyasu F, Itoh K. Efficacy of perflubutane microbubble-enhanced ultrasound in the characterization and detection of focal liver lesions: phase 3 multicenter clinical trial. *AJR Am J Roentgenol.* 2009;193:86-95. [crossref](#)
  101. Bruix J, Sherman M; American Association for the Study of Liver Diseases. Management of hepatocellular carcinoma: an update. *Hepatology.* 2011;53:1020-2. [crossref](#)
  102. Chen LD, Xu HX, Xie XY, Xie XH, Xu ZF, Liu GJ, et al. Intrahepatic cholangiocarcinoma and hepatocellular carcinoma: differential diagnosis with contrast-enhanced ultrasound. *Eur Radiol.* 2010;20:743-53. [crossref](#)
  103. Liu GJ, Wang W, Lu MD, Xie XY, Xu HX, Xu ZF, et al. Contrast-enhanced ultrasound for the characterization of hepatocellular carcinoma and intrahepatic cholangiocarcinoma. *Liver Cancer.* 2015;4:241-52. [crossref](#)
  104. Xu HX, Chen LD, Liu LN, Zhang YF, Guo LH, Liu C. Contrast-enhanced ultrasound of intrahepatic cholangiocarcinoma: correlation with pathological examination. *Br J Radiol.* 2012;85:1029-37. [crossref](#)
  105. Xu HX, Lu MD, Liu GJ, Xie XY, Xu ZF, Zheng YL, et al. Imaging of peripheral cholangiocarcinoma with low-mechanical index contrast-enhanced sonography and SonoVue: initial experience. *J Ultrasound Med.* 2006;25:23-33. [crossref](#)
  106. Claudon M, Cosgrove D, Albrecht T, Bolondi L, Bosio M, Calliada F, et al. Guidelines and good clinical practice recommendations for contrast enhanced ultrasound (CEUS): update 2008. *Ultraschall Med.* 2008;29:28-44. [crossref](#)
  107. Numata K, Luo W, Morimoto M, Kondo M, Kunishi Y, Sasaki T, et al. Contrast enhanced ultrasound of hepatocellular carcinoma. *World J Radiol.* 2010;2:68-82. [crossref](#)
  108. Albrecht T, Blomley M, Bolondi L, Claudon M, Correas JM, Cosgrove D, et al. Guidelines for the use of contrast agents in ultrasound. *Ultraschall Med.* 2004;25:249-56. [crossref](#)
  109. Kong WT, Wang WP, Huang BJ, Ding H, Mao F. Value of wash-in and wash-out time in the diagnosis between hepatocellular carcinoma and other hepatic nodules with similar vascular pattern on contrast-enhanced ultrasound. *J Gastroenterol Hepatol.* 2014;29:576-80. [crossref](#)
  110. Yanagisawa K, Moriyasu F, Miyahara T, Yuki M, Iijima H. Phagocytosis of ultrasound contrast agent microbubbles by Kupffer cells. *Ultrasound Med Biol.* 2007;33:318-25. [crossref](#)
  111. Maruyama H, Sekimoto T, Yokosuka O. Role of contrast-enhanced ultrasonography with Sonazoid for hepatocellular carcinoma: evidence from a 10-year experience. *J Gastroenterol.* 2016;51:421-33. [crossref](#)
  112. von Herbay A, Haeussinger D, Gregor M, Vogt C. Characterization and detection of hepatocellular carcinoma (HCC): comparison of the ultrasound contrast agents SonoVue (BR 1) and Levovist (SH U 508A)—comparison of SonoVue and Levovist in HCC. *Ultraschall Med.* 2007;28:168-75. [crossref](#)
  113. Sidhu PS, Choi BI, Nielsen MB. The EFSUMB Guidelines on the Non-hepatic Clinical Applications of Contrast Enhanced Ultrasound (CEUS): a new dawn for the escalating use of this ubiquitous technique. *Ultraschall Med.* 2012;33:5-7. [crossref](#)
  114. Piscaglia F, Bolondi L, Italian Society for Ultrasound in Medicine and Biology (SIUMB) Study Group on Ultrasound Contrast Agents. The safety of Sonovue in abdominal applications: retrospective analysis of 23188 investigations. *Ultrasound Med Biol.* 2006;32:1369-75. [crossref](#)
  115. ter Haar G. Safety and bio-effects of ultrasound contrast agents. *Med Biol Eng Comput.* 2009;47:893-900. [crossref](#)
  116. The European Agency for the Evaluation of Medicinal Products. Public statement on Sonovue (Sulphur hexafluoride) new contraindication in patients with heart disease: restriction of use to non-cardiac imaging. London: The European Agency for the Evaluation of Medicinal Products; 2014.

117. Piscaglia F, Nolsoe C, Dietrich CF, Cosgrove DO, Gilja OH, Bachmann Nielsen M, et al. The EFSUMB Guidelines and Recommendations on the Clinical Practice of Contrast Enhanced Ultrasound (CEUS): update 2011 on non-hepatic applications. *Ultraschall Med.* 2012;33:33-59. [crossref](#)
118. Xu HX, Liu GJ, Lu MD, Xie XY, Xu ZF, Zheng YL, et al. Characterization of small focal liver lesions using real-time contrast-enhanced sonography: diagnostic performance analysis in 200 patients. *J Ultrasound Med.* 2006;25:349-61. [crossref](#)
119. Xu HX, Liu GJ, Lu MD, Xie XY, Xu ZF, Zheng YL, et al. Characterization of focal liver lesions using contrast-enhanced sonography with a low mechanical index mode and a sulfur hexafluoride-filled microbubble contrast agent. *J Clin Ultrasound.* 2006;34:261-72. [crossref](#)
120. Xu HX, Xie XY, Lu MD, Liu GJ, Xu ZF, Zheng YL, et al. Contrast-enhanced sonography in the diagnosis of small hepatocellular carcinoma < or =2 cm. *J Clin Ultrasound.* 2008;36:257-66. [crossref](#)
121. Quaia E, Calliada F, Bertolotto M, Rossi S, Garioni L, Rosa L, et al. Characterization of focal liver lesions with contrast-specific US modes and a sulfur hexafluoride-filled microbubble contrast agent: diagnostic performance and confidence. *Radiology.* 2004;232:420-30. [crossref](#)
122. Bolondi L, Gaiani S, Celli N, Golfieri R, Grigioni WF, Leoni S, et al. Characterization of small nodules in cirrhosis by assessment of vascularity: the problem of hypovascular hepatocellular carcinoma. *Hepatology.* 2005;42:27-34. [crossref](#)
123. Chen MH, Dai Y, Yan K, Fan ZH, Yin SS, Yang W, et al. The role of contrast-enhanced ultrasound on the diagnosis of small hepatocellular carcinoma ( $\leq 3$ cm) in patients with cirrhosis. *Hepatol Res.* 2006;35:281-8. [crossref](#)
124. Xu HX, Lu MD, Liu LN, Zhang YF, Guo LH, Xu JM, et al. Discrimination between neoplastic and non-neoplastic lesions in cirrhotic liver using contrast-enhanced ultrasound. *Br J Radiol.* 2012;85:1376-84. [crossref](#)
125. Fan ZH, Chen MH, Dai Y, Wang YB, Yan K, Wu W, et al. Evaluation of primary malignancies of the liver using contrast-enhanced sonography: correlation with pathology. *AJR Am J Roentgenol.* 2006;186:1512-9. [crossref](#)
126. Iavarone M, Sangiovanni A, Forzenigo LV, Massironi S, Fraquelli M, Aghemo A, et al. Diagnosis of hepatocellular carcinoma in cirrhosis by dynamic contrast imaging: the importance of tumor cell differentiation. *Hepatology.* 2010;52:1723-30. [crossref](#)
127. Xu HX, Lu MD. The current status of contrast-enhanced ultrasound in China. *J Med Ultrason (2001).* 2010;37:97-106. [crossref](#)
128. Claudon M, Dietrich CF, Choi BI, Cosgrove DO, Kudo M, Nolsøe CP, et al. Guidelines and good clinical practice recommendations for contrast enhanced ultrasound (CEUS) in the liver - update 2012: A WFUMB-EFSUMB initiative in cooperation with representatives of AFSUMB, AIUM, ASUM, FLAUS and ICUS. *Ultrasound Med Biol.* 2013;39:187-210. [crossref](#)
129. Barreiros AP, Piscaglia F, Dietrich CF. Contrast enhanced ultrasound for the diagnosis of hepatocellular carcinoma (HCC): comments on AASLD guidelines. *J Hepatol.* 2012;57:930-2. [crossref](#)
130. Quaia E, Lorusso A, Grisi G, Stacul F, Cova MA. The role of CEUS in the characterization of hepatocellular nodules detected during the US surveillance program—current practices in Europe. *Ultraschall Med.* 2012;33(Suppl 1):S48-56. [crossref](#)
131. Goto E, Masuzaki R, Tateishi R, Kondo Y, Imamura J, Goto T, et al. Value of post-vascular phase (Kupffer imaging) by contrast-enhanced ultrasonography using Sonazoid in the detection of hepatocellular carcinoma. *J Gastroenterol.* 2012;47:477-85. [crossref](#)
132. Ohama H, Imai Y, Nakashima O, Kogita S, Takamura M, Hori M, et al. Images of Sonazoid-enhanced ultrasonography in multistep hepatocarcinogenesis: comparison with Gd-EOB-DTPA-enhanced MRI. *J Gastroenterol.* 2014;49:1081-93. [crossref](#)
133. Kudo M. Hepatocellular carcinoma 2009 and beyond: from the surveillance to molecular targeted therapy. *Oncology.* 2008;75(Suppl 1):1-12. [crossref](#)
134. Hatanaka K, Kudo M, Minami Y, Maekawa K. Sonazoid-enhanced ultrasonography for diagnosis of hepatic malignancies: comparison with contrast-enhanced CT. *Oncology.* 2008;75(Suppl 1):42-7. [crossref](#)
135. Tanaka H, Iijima H, Nouse K, Aoki N, Iwai T, Takashima T, et al. Cost-effectiveness analysis on the surveillance for hepatocellular carcinoma in liver cirrhosis patients using contrast-enhanced ultrasonography. *Hepatol Res.* 2012;42:376-84. [crossref](#)
136. Kim TK, Lee KH, Khalili K, Jang HJ. Hepatocellular nodules in liver cirrhosis: contrast-enhanced ultrasound. *Abdom Imaging.* 2011;36:244-63. [crossref](#)
137. Wu W, Chen MH, Yin SS, Yan K, Fan ZH, Yang W, et al. The role of contrast-enhanced sonography of focal liver lesions before percutaneous biopsy. *AJR Am J Roentgenol.* 2006;187:752-61. [crossref](#)
138. Forner A, Llovet JM, Bruix J. Hepatocellular carcinoma. *Lancet.* 2012;379:1245-55. [crossref](#)
139. Lencioni R. Loco-regional treatment of hepatocellular carcinoma. *Hepatology.* 2010;52:762-73. [crossref](#)
140. Cho YK, Kim JK, Kim MY, Rhim H, Han JK. Systematic review of randomized trials for hepatocellular carcinoma treated with percutaneous ablation therapies. *Hepatology.* 2009;49:453-9. [crossref](#)
141. Xu HX. Era of diagnostic and interventional ultrasound. *World J Radiol.* 2011;3:141-6. [crossref](#)
142. Min JH, Lim HK, Lim S, Kang TW, Song KD, Choi SY, et al. Radiofrequency ablation of very-early-stage hepatocellular carcinoma inconspicuous on fusion imaging with B-mode US: value of fusion imaging with contrast-enhanced US. *Clin Mol Hepatol.* 2014;20:61-70. [crossref](#)
143. Tai CJ, Huang MT, Wu CH, Tai CJ, Shi YC, Chang CC, et al. Contrast-enhanced ultrasound and computed tomography assessment of hepatocellular carcinoma after transcatheter arterial chemo-embolization: a systematic review. *J Gastrointest Liver Dis.* 2016;25:499-507.
144. Xu HX, Lu MD, Xie XH, Xie XY, Kuang M, Xu ZF, et al. Treatment response evaluation with three-dimensional contrast-enhanced ultrasound for liver cancer after local therapies. *Eur J Radiol.* 2010;76:81-8. [crossref](#)
145. Salvaggio G, Campisi A, Lo Greco V, Cannella I, Meloni MF, Caruso G. Evaluation of posttreatment response of hepatocellular carcinoma: comparison of ultrasonography with second-generation ultrasound contrast agent and multidetector CT. *Abdom Imaging.* 2010;35:447-53. [crossref](#)
146. Lu MD, Yu XL, Li AH, Jiang TA, Chen MH, Zhao BZ, et al. Comparison of contrast enhanced ultrasound and contrast enhanced CT or MRI in monitoring percutaneous thermal ablation procedure in patients with hepatocellular carcinoma: a multi-center study in China. *Ultrasound Med Biol.* 2007;33:1736-49. [crossref](#)
147. Andreana L, Kudo M, Hatanaka K, Chung H, Minami Y, Maekawa K, et al. Contrast-enhanced ultrasound techniques for guiding and assessing response to locoregional treatments for hepatocellular carcinoma. *Oncology.* 2010;78(Suppl 1):68-77. [crossref](#)
148. Inoue T, Kudo M, Hatanaka K, Arizumi T, Takita M, Kitai S, et al. Usefulness of contrast-enhanced ultrasonography to evaluate the post-treatment responses of radiofrequency ablation for hepatocellular carcinoma: comparison with dynamic CT. *Oncology.* 2013;84(Suppl 1):51-7. [crossref](#)
149. Lencioni R, Llovet JM. Modified RECIST (mRECIST) assessment for hepatocellular carcinoma. *Semin Liver Dis.* 2010;30:52-60. [crossref](#)

150. Forner A, Ayuso C, Varela M, Rimola J, Hessheimer AJ, de Lope CR, et al. Evaluation of tumor response after locoregional therapies in hepatocellular carcinoma: are response evaluation criteria in solid tumors reliable. *Cancer*. 2009;115:616-23. [cross ref](#)
151. Frieser M, Kiesel J, Lindner A, Bernatik T, Haensler JM, Janka R, et al. Efficacy of contrast-enhanced US versus CT or MRI for the therapeutic control of percutaneous radiofrequency ablation in the case of hepatic malignancies. *Ultraschall Med*. 2011;32:148-53. [cross ref](#)
152. Mauri G, Porazzi E, Cova L, Restelli U, Tondolo T, Bonfanti M, et al. Intraprocedural contrast-enhanced ultrasound (CEUS) in liver percutaneous radiofrequency ablation: clinical impact and health technology assessment. *Insights Imaging*. 2014;5:209-16. [cross ref](#)
153. Kim CK, Choi D, Lim HK, Kim SH, Lee WJ, Kim MJ, et al. Therapeutic response assessment of percutaneous radiofrequency ablation for hepatocellular carcinoma: utility of contrast-enhanced agent detection imaging. *Eur J Radiol*. 2005;56:66-73. [cross ref](#)
154. Zheng SG, Xu HX, Lu MD, Xie XY, Xu ZF, Liu GJ, et al. Role of contrast-enhanced ultrasound in follow-up assessment after ablation for hepatocellular carcinoma. *World J Gastroenterol*. 2013;19:855-65. [cross ref](#)